

# Effect of the Support Shape on Fischer-Tropsch Cobalt Catalyst Performance

Jian Huang, Weixin Qian, Hongfang Ma, Haitao Zhang, Weiyong Ying

**Abstract**—Cobalt catalysts were supported on extruded silica carrier and different-type ( $\text{SiO}_2$ ,  $\gamma\text{-Al}_2\text{O}_3$ ) commercial supports with different shapes and sizes to produce heavy hydrocarbons for Fischer-Tropsch synthesis. The catalysts were characterized by  $\text{N}_2$  physisorption and  $\text{H}_2$ -TPR. The catalytic performance of the catalysts was tested in a fixed bed reactor. The results of Fischer-Tropsch synthesis performance showed that the cobalt catalyst supported on spherical silica supports displayed a higher activity and a higher selectivity to  $\text{C}_5^+$  products, due to the fact that the active components were only distributed in the surface layer of spherical carrier, and the influence of gas diffusion restriction on catalytic performance was weakened. Therefore, it can be concluded that the eggshell cobalt catalyst was superior to precious metals modified catalysts in the synthesis of heavy hydrocarbons.

**Keywords**—Fischer-Tropsch synthesis, cobalt catalyst, support shape, heavy hydrocarbons.

## I. INTRODUCTION

FISCHER-TROPSCH SYNTHESIS (FTS) is a major part of gas (coal and biomass) to liquid fuels, which involves the formation of hydrocarbons from synthesis gas ( $\text{CO}$  and  $\text{H}_2$ ) derived from coal, natural gas, shale gas or biomass through gasification, steam reforming, or partial thermal oxidation [1], [2]. FTS technology is a prospective and environmentally friendly process to produce ultra-clean fuel products without sulfur, nitrogen [3], [4]. At present, cobalt catalyst and iron catalyst have been successfully applied for FTS reaction in industry [2]. Cobalt is considered as the most favorable metal for the synthesis of heavy hydrocarbons, owing to its higher activity, higher selectivity to long chain paraffin, higher resistance toward deactivation, and lower water gas shift activity than iron [5]. The activity and selectivity of FTS catalyst is determined by the active metal, promotor, and support, to a large extent.

Recently, cobalt catalysts have acquired a great intention, due to its high selectivity to heavy hydrocarbons. In general, cobalt catalysts were anchored on inert supports, such as  $\text{Al}_2\text{O}_3$  [6],  $\text{SiO}_2$  [7], zeolite [8], and carbon materials [9]. Moreover,

transition metal oxides were also used as supports, such as  $\text{ZrO}_2$  [10],  $\text{TiO}_2$  [11], and  $\text{CeO}_2$  [12]. The modification of cobalt catalysts has been widely performed by the addition of transition metal and noble metal, such as Zr [13], La [14], Nb [15], and Ru [16].

However, the shape and pellet size of cobalt catalysts are seriously affected the activity and selectivity of FTS reaction. In industrial fixed-bed reactors, cobalt catalysts are always prepared as fine crystalline nanoparticles anchored on a thermally stable, chemically inert porous support with a diameter of 1-3 mm for maintaining a reasonable pressure drop [17]. During typical FTS reaction, the pores of the catalyst pellet are filled with hydrocarbon liquid, therefore, reactant gases have to dissolve in the liquid and diffuse into the porous pellet surface to react on the active metal sites to synthesis product in liquid and gases phases, which then have to diffuse out through the liquid filled pores [18]. This presents that the active metal particles located deep in the interior of the catalyst pellet are less effective than those near the pellet exterior. In this regard, particles smaller than 0.2 mm have been suggested to overcome diffusion limitations [19].

The aim of this work is to investigate the effect of the support shape on cobalt catalysts supported on silica or alumina in FTS reaction. The cobalt catalyst modified by Nb, Ru, Zr, or La was prepared by two-step impregnation method and tested in a fixed tube reactor to analyze support shape effect on activity, products selectivity and products distribution. The texture, reduction properties, and FTS catalytic performance of cobalt catalysts were researched via  $\text{N}_2$  physisorption, X-ray diffraction (XRD), and  $\text{H}_2$  temperature-programmed reduction ( $\text{H}_2$ -TPR).

## II. EXPERIMENTAL

### A. Preparation of Catalysts

A series of cobalt catalysts were prepared by impregnation on extruded silica carrier and different-type ( $\text{SiO}_2$ ,  $\gamma\text{-Al}_2\text{O}_3$ ) commercial supports with different shape and size and employed by different promoters. The cobalt catalysts were supported on silica pellet (average diameter = 2.2 mm), extruded silica (diameter = 2 mm), wheel-shaped alumina (diameter = 5 mm), spherical alumina (average diameter = 1.7 mm), and trifoliate alumina (equivalent diameter = 1.5 mm), respectively, as shown in Fig. 1. Cobalt (II) nitrate hexahydrate (>99 wt.% Sinopharm Chemical Reagent Co., Ltd), zirconium nitrate (>99.5 wt.% Sinopharm Chemical Reagent Co., Ltd), lanthanum nitrate (>99 wt.% Sinopharm Chemical Reagent Co., Ltd), ruthenium chloride (>99 wt.% Sinopharm Chemical Reagent Co., Ltd), and niobium oxalates (> 99.99 wt.%,

Weixin Qian, Hongfang Ma and Haitao Zhang are with Engineering Research Center of Large Scale Reactor Engineering and Technology, Ministry of Education, State Key Laboratory of Chemical Engineering, the East China University of Science and Technology, Shanghai, 200237 China.

Jian Huang is with Engineering Research Center of Large Scale Reactor Engineering and Technology, Ministry of Education, State Key Laboratory of Chemical Engineering, the East China University of Science and Technology, Shanghai, 200237 China (e-mail: jhecust@hotmail.com).

Weiyong Ying is with Engineering Research Center of Large Scale Reactor Engineering and Technology, Ministry of Education, State Key Laboratory of Chemical Engineering, the East China University of Science and Technology, Shanghai, 200237 China (corresponding author, e-mail: wyying@ecust.edu.cn).

Guangdong Weng Jiang Chemical Reagent Co., Ltd.) were supported on the pellets via two step impregnation method. After the impregnation step, the catalysts were dried at 110 °C for 12 h, followed by calcination in air at 400 °C for 6 h. The obtained catalysts were denoted as Co-Ru/Zr-SiO<sub>2</sub>-Extrusion, Co/Nb-SiO<sub>2</sub>-Eggshell, Co/Nb-Al<sub>2</sub>O<sub>3</sub>-Sphere, Co-Ru/La-Zr-Al<sub>2</sub>O<sub>3</sub>-Trefoil, and Co-Ru/La-Zr-Al<sub>2</sub>O<sub>3</sub>-Wheel.



Fig. 1 Different shape of supports: (a) SiO<sub>2</sub>-Sphere (d=2.2 mm), (b) cross section of eggshell catalyst (Co/Nb-SiO<sub>2</sub>-Eggshell, d=2.2 mm, Δd=120~160 μm), (c) SiO<sub>2</sub>-Extrusion (d=2.0 mm), (d) Al<sub>2</sub>O<sub>3</sub>-Sphere (d=1.7 mm), (e) Al<sub>2</sub>O<sub>3</sub>-Wheel (d=5.0 mm), and (f) Al<sub>2</sub>O<sub>3</sub>-Trefoil (d=1.5 mm)

### B. Characterization of Catalysts

N<sub>2</sub> physisorption were obtained with a Micrometrics ASAP 2020 apparatus. Prior to N<sub>2</sub> adsorption, the samples were degassed under vacuum at 350 °C for 4 h. Specific surface areas were measured by Brunauer Emmett Teller (BET) method. Total pore volume and pore sizes were evaluated using the standard Barrett-Joyner-Halenda (BJH) treatment.

Powder x-ray diffraction (XRD) patterns were recorded on a Rigaku D/Max 2550 using Cu Kα radiation at 40 kV and 100 mA. XRD patterns were obtained over a 2θ range of 10~80° and a step size of 0.02°.

Hydrogen temperature-programmed reduction (H<sub>2</sub>-TPR) measurements were carried out on Micrometrics AutoChem II 2920. Prior to the measurements, about 50 mg catalyst sample was purged in a flow of Argon at 350 °C for 2.0 h, and then cooled to 50 °C. Each sample was treated in 10 % H<sub>2</sub>/90 % Ar (v/v) at a flow rate of 30 ml·min<sup>-1</sup> under atmospheric pressure. Hydrogen consumption was measured by a thermal conductivity detector (TCD) with a heating rate of 10 °C·min<sup>-1</sup>.

### C. Test of Catalyst Performance

The performance of samples was tested in a fixed-bed reactor (ID 12 mm). The weight of the sample was 3.0 g mixed. All catalysts were reduced under the atmosphere of pure H<sub>2</sub>, pressure at 0.1 MPa, temperature at 400 °C, space velocity at

1000 cm<sup>3</sup>(STP) g<sup>-1</sup> h<sup>-1</sup>, for 24 h. The reaction conditions were kept at 2.0~3.8 MPa, 210~220 °C, 850~2000 cm<sup>3</sup> (STP) g<sup>-1</sup> h<sup>-1</sup> in the reaction system. The reactor apparatus and the product analysis system had been described in previous studies [20]. This work just took alkanes into consideration and neglected aromatic compounds, alcohols and other oxygen containing compounds. X<sub>CO</sub> represents the conversion of CO and can be calculated by

$$X_{CO}(\%) = \frac{N_{CO,in} - N_{CO,out}}{N_{CO,in}} \times 100 \quad (1)$$

S<sub>C<sub>n</sub></sub> represents the selectivity of C<sub>n</sub> hydrocarbons and can be calculated by

$$S_{C_n}(\%) = \frac{n \cdot N_{C_n,out}}{N_{CO,in} - N_{CO,out}} \times 100 \quad (2)$$

WGS reaction can be calculated by

$$S_{CO_2}(\%) = \frac{N_{CO_2,out}}{N_{CO,in} - N_{CO,out}} \times 100 \quad (3)$$

N is the mole flow rate (mol·h<sup>-1</sup>), and n is the carbon number of hydrocarbons.

## III. RESULTS AND DISCUSSION

The N<sub>2</sub> adsorption-desorption isotherms are shown in Fig. 2. All the isotherms present a typical type IV curve, which was characteristic of mesoporous material. the pore size distribution of the catalysts is presented in Fig. 3. Co/Nb-SiO<sub>2</sub>-Eggshell has the widest pore size distribution, about 5~45 nm.

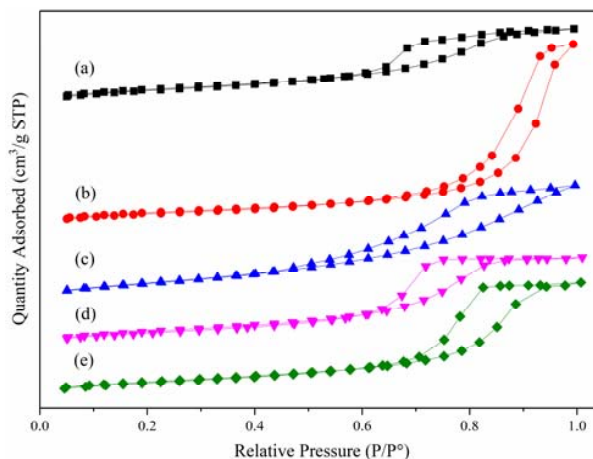


Fig. 2 N<sub>2</sub> adsorption-desorption isotherm of the catalysts: (a) Co-Ru/Zr-SiO<sub>2</sub>-Extrusion, (b) Co/Nb-SiO<sub>2</sub>-Eggshell, (c) Co/Nb-Al<sub>2</sub>O<sub>3</sub>-Sphere, (d) Co-Ru/La-Zr-Al<sub>2</sub>O<sub>3</sub>-Trefoil, (e) Co-Ru/La-Zr-Al<sub>2</sub>O<sub>3</sub>-Wheel

A brief compilation of the textural properties of the catalysts is presented in Table I. As observed, the pore volume and average pore diameter of Co/Nb-SiO<sub>2</sub>-Eggshell is larger than

that of other samples, but its surface area is the smallest.

TABLE I  
SURFACE AREA, PORE VOLUME, AND AVERAGE PORE DIAMETER FOR FRESH CALCINED CATALYSTS

Sample	$S_{\text{BET}}$ ( $\text{m}^2 \cdot \text{g}^{-1}$ )	$V_p^a$ ( $\text{cm}^3 \cdot \text{g}^{-1}$ )	$D_p^b$ (nm)
Co-Ru/Zr-SiO <sub>2</sub> -Extrusion	129.1	0.22	5.7
Co/Nb-SiO <sub>2</sub> -Eggshell	119.5	0.51	14.0
Co/Nb-Al <sub>2</sub> O <sub>3</sub> -Sphere	179.9	0.34	5.8
Co-Ru/La-Zr-Al <sub>2</sub> O <sub>3</sub> -Trefoil	144.4	0.27	6.0
Co-Ru/La-Zr-Al <sub>2</sub> O <sub>3</sub> -Wheel	132.3	0.32	8.0

<sup>a</sup> BJH desorption pore volume.

<sup>b</sup> Adsorption average pore.

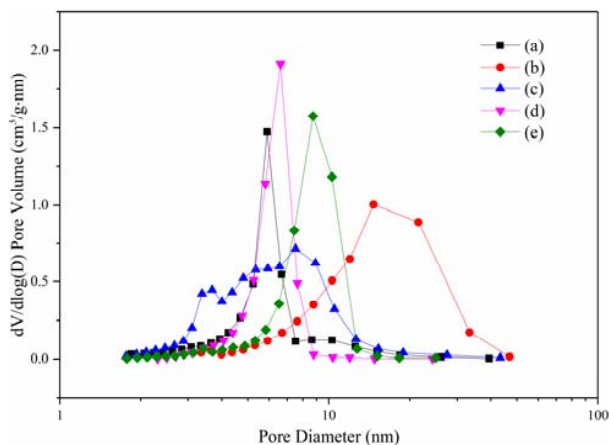


Fig. 3 The pore size distributions of the catalysts: (a) Co-Ru/Zr-SiO<sub>2</sub>-Extrusion, (b) Co/Nb-SiO<sub>2</sub>-Eggshell, (c) Co/Nb-Al<sub>2</sub>O<sub>3</sub>-Sphere, (d) Co-Ru/La-Zr-Al<sub>2</sub>O<sub>3</sub>-Trefoil, (e) Co-Ru/La-Zr-Al<sub>2</sub>O<sub>3</sub>-Wheel

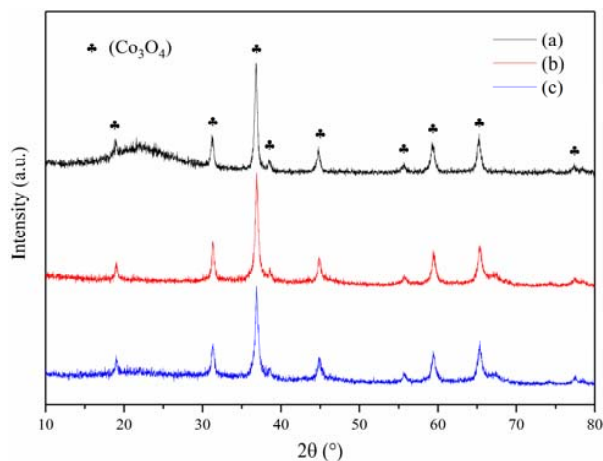


Fig. 4 XRD patterns of fresh calcined catalysts: (a) Co-Ru/Zr-SiO<sub>2</sub>-Extrusion, (b) Co/Nb-Al<sub>2</sub>O<sub>3</sub>-Sphere, (c) Co-Ru/La-Zr-Al<sub>2</sub>O<sub>3</sub>-Trefoil

The XRD patterns of the cobalt catalysts are employed, as displayed in Fig. 4. The main diffraction peaks at  $2\theta = 19.0^\circ$ ,  $31.2^\circ$ ,  $36.8^\circ$ ,  $44.8^\circ$ ,  $55.6^\circ$ ,  $59.3^\circ$  and  $65.2^\circ$  are assigned to Co<sub>3</sub>O<sub>4</sub> spinel, according to the JCPDS cards (no. 43-1003), but

no peaks corresponding to ZrO<sub>2</sub>, RuO<sub>2</sub>, La<sub>2</sub>O<sub>3</sub>, and Nb<sub>2</sub>O<sub>5</sub> were obviously observed. The noise levels have suggested that the support of catalysts is amorphous. However, all of these catalysts have the same phase, cubic Co<sub>3</sub>O<sub>4</sub>.

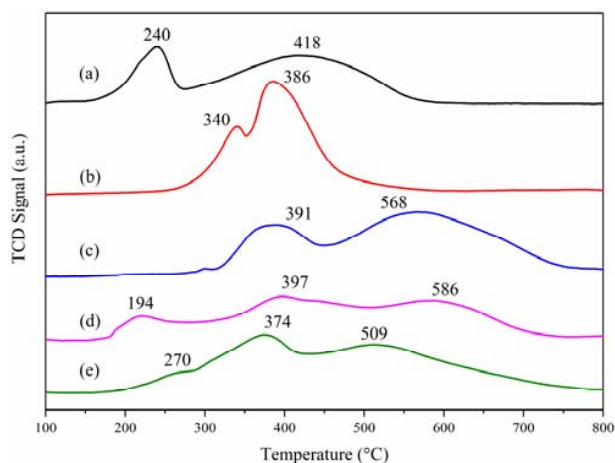


Fig. 5 H<sub>2</sub>-TPR profiles of the two fresh calcined cobalt catalysts: (a) Co-Ru/Zr-SiO<sub>2</sub>-Extrusion, (b) Co/Nb-SiO<sub>2</sub>-Eggshell, (c) Co/Nb-Al<sub>2</sub>O<sub>3</sub>-Sphere, (d) Co-Ru/La-Zr-Al<sub>2</sub>O<sub>3</sub>-Trefoil, (e) Co-Ru/La-Zr-Al<sub>2</sub>O<sub>3</sub>-Wheel

The reduction patterns of cobalt catalysts are performed in two steps as follows:  $\text{Co}^{3+} \rightarrow \text{Co}^{2+}$ , and  $\text{Co}^{2+} \rightarrow \text{Co}^0$  [2]. The H<sub>2</sub>-TPR profiles of the samples are shown in Fig. 5. For silica supported catalysts, the first reduction peak at 240 °C is ascribed to the reduction of Co<sup>3+</sup> to Co<sup>2+</sup> and the reduction of RuO<sub>2</sub> to metal Ru for Co-Ru/Zr-SiO<sub>2</sub>-Extrusion. The second reduction peaks at 418 °C and 386 °C are attributed to the reduction of Co<sup>2+</sup> to metal Co. The high reduction temperature of Co-Ru/Zr-SiO<sub>2</sub>-Extrusion is higher than that of Co/Nb-SiO<sub>2</sub>-Eggshell, due to the fact that Co-Ru/Zr-SiO<sub>2</sub>-Extrusion has a smaller pore size and stronger metal support interaction. The active metal of Co/Nb-SiO<sub>2</sub>-Eggshell is located on the surface layer of the silica sphere, so that it has a lower metal support interaction and mass transfer limitation.

As to alumina supported catalysts, the reduction peak at 194 °C and 270 °C is ascribed to the reduction of RuO<sub>2</sub> on catalysts surface. And the reduction peaks at 374 °C, 391 °C, and 397 °C are attributed to the reduction of Co<sup>3+</sup> to Co<sup>2+</sup>. The reduction peaks at 568 °C, 586 °C, and 505 °C are ascribed to the reduction of Co<sup>2+</sup> to metal Co. In comparison with silica supported catalysts, alumina supported catalysts have a stronger metal support interaction, resulting in a higher reduction temperature.

The FTS performance of catalysts for was obtained in a fixed bed after 48 h. The reaction condition and the reaction results are listed in Table II. The results indicated that the catalyst Co-Ru/Zr-SiO<sub>2</sub>-Extrusion had a higher FTS performance, on which the CO conversion was 42.6 % and the selectivity to CH<sub>4</sub> and C<sub>5</sub><sup>+</sup> products was 11.5% and 80.7%, respectively. The Co/Nb-SiO<sub>2</sub>-Eggshell sample was superior to precious metals-modified catalysts in the synthesis of heavy hydrocarbons, on which the CO conversion was 75.4% and the selectivity to CH<sub>4</sub> and C<sub>5</sub><sup>+</sup> products was 7.0% and 86.7%, respectively. Therefore,

eggshell cobalt catalyst has a superior performance of FTS reaction because the influence of gas diffusion restriction on catalytic performance was weakened. When the ratio of  $H_2/CO$  was 2.0, the  $CH_4$  selectivity of alumina supported samples was higher than 13%, even up to 25.6%. Thus, for alumina supported catalysts, the selectivity to  $CH_4$  is significantly higher than silica supported samples, owing to its stronger

metal support interaction and forming more methane production activity sites during the reduction process. When the syngas with low ratio of  $H_2/CO$  over Co-Ru/La-Zr- $Al_2O_3$ -Trefoil was introduced in reactor, the selectivity to  $CH_4$  was significantly diminished, down to 6.2%, while the selectivity to  $C_5^+$  products was remarkable increased, up to 84.3%.

TABLE II  
FTS CATALYTIC PERFORMANCE OF INDUSTRIAL PARTICLE CATALYSTS WITH DIFFERENT SHAPES<sup>a</sup>

Catalyst	Reaction Condition				Xco	Selectivity <sup>b</sup> (%)			
	T (°C)	P (MPa)	SV <sup>a</sup>	H <sub>2</sub> /CO ratio	%	CO <sub>2</sub>	CH <sub>4</sub>	C <sub>2-4</sub>	C <sub>5</sub> <sup>+</sup>
Co-Ru/Zr-SiO <sub>2</sub> -Extrusion	210	3.0	850	2.0	77.4	1.1	10.0	5.6	83.3
Co/Nb-SiO <sub>2</sub> -Eggshell	200	3.8	1000	2.0	75.4	1.0	7.0	5.3	86.7
Co/Nb-Al <sub>2</sub> O <sub>3</sub> -Sphere	220	3.0	1000	2.0	57.9	2.2	20.2	8.7	68.9
Co-Ru/La-Zr-Al <sub>2</sub> O <sub>3</sub> -Trefoil	200	2.0	1000	2.0	62.9	1.0	13.1	7.0	78.9
	200	2.0	1000	1.2	31.8	1.1	6.2	8.4	84.3
Co-Ru/La-Zr-Al <sub>2</sub> O <sub>3</sub> -Wheel	200	3.8	2000	2.0	37.8	1.1	25.6	12.6	60.7

<sup>a</sup>The catalytic activity and product selectivity data were calculated by averaging the values of 24 h.

<sup>b</sup>The data were based on mole carbon atom.

#### IV. CONCLUSION

A series of cobalt catalysts supported on different shape carriers were prepared by impregnation method, and its texture properties and reduction properties were characterized by BET, XRD, and  $H_2$ -TPR. The test results showed that the cobalt catalyst supported on spherical silica carrier presented a higher selectivity to  $C_5^+$  products and higher FTS activity. The Co/Nb-SiO<sub>2</sub>-Eggshell sample was superior to precious metals-modified catalysts in the synthesis of heavy hydrocarbons, due to its lower metal support interaction and mass transfer limitation. In comparison with silica supported catalysts, alumina supported catalysts have a stronger metal support interaction, resulting in a higher reduction temperature. In the meanwhile, the cobalt catalyst anchored on trefoil support also facilitated the synthesis of heavy hydrocarbons and inhibited the production of  $CH_4$ .

#### ACKNOWLEDGMENT

The authors gratefully acknowledge the financial support of the National High-Tech R&D Program of China (2011AA05A204).

#### REFERENCES

- [1] E. Iglesia, S. L. Soled, R. A. Fiato, "Fischer-Tropsch synthesis on cobalt and ruthenium. Metal dispersion and support effects on reaction rate and selectivity." *J. Catal.* Vol. 137, no. 1, pp. 212-224, 1992.
- [2] A. Y. Khodakov, W. Chu, P. Fongarland, "Advances in the development of novel cobalt Fischer-Tropsch catalysts for synthesis of long-chain hydrocarbons and clean fuels." *Chem. Rev.* Vol. 107, no. 5, pp. 1692-1744, 2007.
- [3] K. Srirangan, L. Akawi, M. Moo-Young, C. P. Chou, "Towards sustainable production of clean energy carriers from biomass resources." *Appl. Energ.* Vol. 100, no. 8, pp. 172-186, 2012.
- [4] H. Xiong, L. L. Jewell, N. J. Coville, "Shaped Carbons As Supports for the Catalytic Conversion of Syngas to Clean Fuels." *ACS Catal.* Vol. 5, no. 4, pp. 2640-2658, 2015.
- [5] A. Griboval-Constant, A. Butel, V. V. Ordonsky, P. A. Chernavskii, A. Y. Khodakov, "Cobalt and iron species in alumina supported bimetallic catalysts for Fischer-Tropsch reaction." *Appl. Catal. A: Gen.* Vol. 481, no., pp. 116-126, 2014.
- [6] M. J. Parnian, A. Taheri Najafabadi, Y. Mortazavi, A. A. Khodadadi, I. Nazzari, "Ru promoted cobalt catalyst on  $\gamma$ - $Al_2O_3$ : Influence of different catalyst preparation method and Ru loadings on Fischer-Tropsch reaction and kinetics." *Appl. Surf. Sci.* Vol. 313, no., pp. 183-195, 2014.
- [7] J. Huang, W. Qian, H. Zhang, W. Ying, "Investigation on Fischer-Tropsch Synthesis over Cobalt-Gadolinium Catalyst." *World Academy of Science, Engineering and Technology, International Journal of Chemical and Molecular Engineering* Vol. 10, no. 8, pp. 1042-1045, 2016.
- [8] J. Huang, W. Qian, H. Zhang, W. Ying, "Influences of ordered mesoporous silica on product distribution over Nb-promoted cobalt catalyst for Fischer-Tropsch synthesis." *Fuel* Vol. 216, no., pp. 843-851, 2018.
- [9] T. O. Eschemann, W. S. Lamme, R. L. Manchester, T. E. Parmentier, A. Cognigni, M. Rønning, K. P. de Jong, "Effect of support surface treatment on the synthesis, structure, and performance of Co/CNT Fischer-Tropsch catalysts." *J. Catal.* Vol. 328, no., pp. 130-138, 2015.
- [10] X. Zhang, H. Su, Y. Zhang, X. Gu, "Effect of  $CeO_2$  promotion on the catalytic performance of Co/ZrO<sub>2</sub> catalysts for Fischer-Tropsch synthesis." *Fuel* Vol. 184, no., pp. 162-168, 2016.
- [11] T. O. Eschemann, K. P. de Jong, "Deactivation Behavior of Co/TiO<sub>2</sub> Catalysts during Fischer-Tropsch Synthesis." *ACS Catal.* Vol. 5, no., pp. 3181-3188, 2015.
- [12] L. Spadaro, F. Arena, M. Granados, M. Ojeda, J. Fierro, F. Frusteri, "Metal-support interactions and reactivity of Co/ $CeO_2$  catalysts in the Fischer-Tropsch synthesis reaction." *J. Catal.* Vol. 234, no. 2, pp. 451-462, 2005.
- [13] H. Wu, Y. Yang, H. Suo, M. Qing, L. Yan, B. Wu, J. Xu, H. Xiang, Y. Li, "Effects of ZrO<sub>2</sub> promoter on physico-chemical properties and activity of Co/TiO<sub>2</sub>-SiO<sub>2</sub> Fischer-Tropsch catalysts." *J. Mol. Catal. A: Chem.* Vol. 396, no., pp. 108-119, 2015.
- [14] Z. Cai, J. Li, K. Liew, J. Hu, "Effect of La<sub>2</sub>O<sub>3</sub>-doping on the  $Al_2O_3$  supported cobalt catalyst for Fischer-Tropsch synthesis." *J. Mol. Catal. A: Chem.* Vol. 330, no. 1-2, pp. 10-17, 2010.
- [15] J. Huang, W. Qian, H. Zhang, W. Ying, "In situ investigation on Co-phase evolution and its performance for Fischer-Tropsch synthesis over Nb-promoted cobalt catalysts." *Catal. Sci. Technol.* Vol. 7, no. 23, pp. 5530-5539, 2017.
- [16] M. A. Coronel-García, A. I. Reyes de la Torre, J. A. Melo-Banda, A. L. Martínez-Salazar, R. Silva Rodrigo, N. P. Díaz Zavala, B. Portales Martínez, J. M. Domínguez, "Study of Co, Ru/SBA-15 type materials for Fischer-Tropsch synthesis in fixed bed tubular reactor: I. Effect of the high Ru content on the catalytic activity." *Int. J. Hydrogen. Energ.* Vol. 40, no. 48, pp. 17264-17271, 2015.
- [17] M. F. M. Post, A. C. V. T. Hoog, J. K. Minderhoud, S. T. Sie, "Diffusion limitations in Fischer-Tropsch catalysts." *AIChE J.* Vol. 35, no. 7, pp. 1107-1114, 1989.
- [18] S. A. Gardezi, J. T. Wolan, B. Joseph, "Effect of catalyst preparation conditions on the performance of eggshell cobalt/SiO<sub>2</sub> catalysts for

- Fischer-Tropsch synthesis." *Appl. Catal. A: Gen* Vol. 447-448, no., pp. 151-163, 2012.
- [19] W. H. Zimmerman, J. A. Rossin, D. B. Bukur, "Effect of particle size on the activity of a fused iron Fischer-Tropsch catalyst." *Ind. Eng. Chem. Res.* Vol. 28, no. 4, pp. 406-413, 1989.
- [20] J. Huang, W. Qian, H. Ma, H. Zhang, W. Ying, "Highly selective production of heavy hydrocarbons over cobalt-graphene-silica nanocomposite catalysts." *RSC Advances* Vol. 7, no. 53, pp. 33441-33449, 2017.